Scholars' Mine

Summer 2013

A new approach to nuclear safeguard enhancement through radionuclide profiling

Aaron Dawon Peterson

A NEW APPROACH TO NUCLEAR FUEL SAFEGUARD ENHANCEMENT

THROUGH RADIONUCLIDE PROFILING

by

AARON DAWON PETERSON

A THESIS

Presented to the Faculty of the Graduate School of the

MISSOURI UNIVERSITY OF SCIENCE AND TECHNOLOGY

In Partial Fulfillment of the Requirements of the Degree

MASTER OF SCIENCE IN NUCLEAR ENGINEERING

2013

Approved by

Ayodeji B. Alajo, Advisor
Carlos H. Castano
Joshua L. Rovey

ABSTRACT

The United States has led the effort to promote peaceful use of nuclear power amongst states actively utilizing it as well as those looking to deploy the technology in the near future. With the attraction being demonstrated by various countries towards nuclear power comes the concern that a nation may have military aspirations for the use of nuclear energy. The International Atomic Energy Agency (IAEA) has established nuclear safeguard protocols and procedures to mitigate nuclear proliferation. The work herein proposed a strategy to further enhance existing safeguard protocols by considering safeguard in nuclear fuel design. The strategy involved the use of radionuclides to profile nuclear fuels. Six radionuclides were selected as identifier materials. The decay and transmutation of these radionuclides were analyzed in reactor operation environment. MCNPX was used to simulate a reactor core. The perturbation in reactivity of the core due to the loading of the radionuclides was insignificant. The maximum positive and negative reactivity change induced was at day 1900 with a value of 0.00185 ± 0.00256 and at day 2000 with -0.00441 ± 0.00249, respectively. The mass of the radionuclides were practically unaffected by transmutation in the core; the change in radionuclide inventory was dominated by natural decay. The maximum material lost due to transmutation was 1.17% in Eu154. Extraneous signals from fission products identical to the radionuclide compromised the identifier signals. Eu154 saw a maximum intensity change at EOC and 30 days post-irradiation of 1260% and 4545%, respectively. Cs137 saw a minimum change of 12% and 89%, respectively. Mitigation of the extraneous signals is cardinal to the success of the proposed strategy. The predictability of natural decay provides a basis for the characterization of the signals from the radionuclide.

ACKNOWLEDGEMENTS

TABLE OF CONTENTS

LIST OF ILLUSTRATIONS

LIST OF TABLES

1. INTRODUCTION

1.1 BACKGROUND

Nuclear energy technology is becoming very attractive to many countries around the world. The promise of energy security and reduced reliance on fossil fuel is a major driver for the renewed interest in nuclear energy. The attraction to this technology is a positive development with regards to the expansion of the industry. However, it also creates concerns of abuse from countries with clandestine intentions.

There has been consideration that countries with genuine interest in pursuing nuclear technology for peaceful application be supported by countries with the technical know-how. Under this proposal, countries seeking nuclear energy (receiving state) will be supplied with nuclear reactors appropriate for the desired purpose [1][2]. The technology supplier would be responsible for the installation, maintenance and retrieval of the nuclear components at the end of life. In the case of a power reactor, retrieval of spent fuel may not be immediate. The spent fuel will require some cooling time. During the cooling period, it is important to safeguard the spent fuel inventory. This is particularly true in a situation where the fuel is entrusted to the receiving state during the cooling period. Such trust implicitly assumes that the receiving state will keep watch over the inventory, and that it will not attempt a diversion of the spent fuel for nuclear proliferation and arms development purposes.

1.1.1 Nuclear Non-proliferation and Safeguard. At the end of World War II, the United States and the Soviet Union emerged as the world's superpowers. Competition arose among these two powers and their allies. With this competition was

the birth of the Nuclear Arms Race. During this time, each nation was stockpiling nuclear weapons and producing nuclear warheads with the capability to totally annihilate the other; which led to a situation termed Mutual Assured Destruction (MAD) because an attack on the enemy would ensure a counterattack [3]. This stalemate helped keep each side from attacking the other. The rest of the world saw the delicate relationship between the United States and the Soviet Union, and feared that having more nuclear states would be even less secure. Due to this concern, the Non Proliferation Treaty (NPT) was introduced and opened for signatures in 1968. The purpose of the NPT was to prevent the spread of nuclear weapon technology to other nations [4]. It became necessary to develop safeguards to prevent nuclear proliferation.

Nuclear safeguards are ways to ensure that non nuclear weapon states are not using their nuclear material for weapons proliferation [5]. By increasing the likelihood of early detection, safeguards deter the non nuclear state from using nuclear material for nefarious purposes. Current safeguard measures include a full range inspection by the International Atomic Energy Agency (IAEA). Nuclear facility operators are required to keep detailed, accurate records of the movement of nuclear materials. Video surveillance and on-site inspections are also used to ensure the location of the nuclear fuel [5]. The IAEA has recently started a push towards Safeguard-by-Design (SBD) for new nuclear facilities. The IAEA describes the SBD approach as one in which "international safeguards are fully integrated into the design process of a new nuclear facility from the initial planning through design, construction, operation, and decommissioning". The goal is to implement the international safeguards more effectively and efficiently [6]. This

also may include designing the safeguard as part of the nuclear material itself. In the case of power reactors, the safeguard could be designed as part of the fuel.

1.1.2 Special Nuclear Materials Handling in Light Water Reactor (LWR) Systems. Light water reactors (LWRs) generally use uranium as its fuel. Before going through the core of a LWR, the uranium has to be enriched and fabricated into fuel. It is necessary that the uranium enrichment is between 2% and 4% by weight of U^{235}. After enrichment, the uranium is fabricated into ceramic fuel pellets and placed in the fuel rods which are then arranged in a fuel assembly [7]. The fuel is then placed in the core and burned, after which the spent fuel would be taken out of the core and placed in an on-site water pool to cool for as long as 20 years before final disposal [7]. In the case of a nation seeking to pursue peaceful use of nuclear power, the enriched fuel will be provided to the nation by an existing nuclear state. However, the nation would be responsible for storing and safeguarding the spent fuel during the cooling period. During this nuclear fuel cycle, a nation intent on diverting fuel for proliferation or a would-be rogue nation has opportunities to steal the fuel. Nations with such clandestine intent are not likely to engage in overt diversion of fuel material due to the current safeguards in place. However, covert diversion would be likely. Such states would be more likely to avoid suspicion by stealing a few fuel rods from an assembly for diversion if they are secretly pursuing nuclear proliferation.

1.1.3 Pressurized Water Reactor (PWR) Systems. Of the 437 power reactors in the world, 357 of those are LWRs [7][8]. Out of the LWRs, there are 273 pressurized water reactors (PWRs) [8]. After World War II, research was being conducted in the use of nuclear technology in power production and naval propulsion. The United States focused on LWR designs which led to the development of the PWR design [9]. The PWR is characterized by having a primary and secondary loop. The primary loop contains pressurized water which goes through the core and contains some radioactivity. The secondary loop contains non radioactive water and steam which turns the turbines. Both loops meet in the steam generator where the heat from the water in the primary loop is transferred to the water in the secondary loop which generate steam [7]. A nation looking to embrace nuclear power would most likely start with a PWR system as it is the most established of all reactor designs. Moreover, the abundance of this reactor type makes the PWR system a candidate in the development of a strategy that will enhance nuclear safeguards and non-proliferation.

1.2 RESEARCH OBJECTIVE AND APPROACH

The objective of this project is to explore the viability of using certain radionuclides for unique identification of nuclear fuels from fabrication to disposal or reprocessing. This effort is focused on the implementation of an identification strategy in PWR fuel assemblies. Particularly in a case where the fuels are supplied to a state that is apparently pursuing nuclear power for peaceful use, it is nearly impossible to accurately judge the intentions of such state. However, activities indicative of adverse use of nuclear materials could be monitored in a timely manner. To achieve this, it is imperative to develop strategies that significantly improve material accountancy. The

approach proposed in this project is to have the fuel safeguard designed as part of the fuel at the time of fabrication. This approach seeks to minimize reliance on overlaid Material Control & Accountancy (MC&A) strategies such as number tags, video surveillance, and physical inspection. Through this strategy, a missing fuel assembly or one that has been tampered with would be identified within reasonable time before any diversion could result in special material recovery by the perpetrators. In order to achieve the objective stated above, the following tasks were completed:

1. Selection criteria for candidate radionuclides that would be effective tracers and signal generators for fuel tagging in this strategy

2. Determination of the effectiveness of tagging materials particularly during reactor operation and post irradiation.

3. Determination of the impact of tagging materials on current reactor operation and safety standards.

The first task was accomplished by establishing selection criteria based on desirable properties of a candidate radionuclide and the selection was made through the review of nuclear data files and cross sections. The second and third tasks were completed through the use of Monte Carlo N-Particle Transport Code (MCNP). The code was used to run the simulations of a PWR core with the nuclear safeguard designed as part of the fuel. The reactor core was modeled based on a Westinghouse AP1000 core configuration, which was designed to operate at a temperature and pressure of 573K and 155 bars, respectively. It should be noted that unlike AP1000, the fresh fuel composition in the PWR modeled was uniform core-wide at 5 percent ^{235}U enrichment. The reactor

criticality calculations were performed using MCNP5 and core burn up calculations were performed with MCNPX2.7.0. The core was run at a constant power of 1100 MW.[10] The uranium dioxide (UO_2) fuel and the identifier were burned in the core for a total of 2200 days. There were nine time steps of 200 days and four time steps of 100 days.

2. DETERMINATION OF TAGGING RADIONUCLIDES

The proposed strategy involved the use of radionuclides in the tagging and monitoring of nuclear fuel assemblies. Through the radionuclide tags, any assembly would be uniquely identified and its history could be retraced. For such a strategy to be successful, the nature and/or denaturing of the radionuclide must lend itself to accurate profiling. The buildup or depletion of signals generated by these radionuclides must be traceable. In this method, combinations of concentrations, concentration changes, activity ratios and other metrics could be used to establish unique tags to any fuel assembly being supplied to a receiving state. In this work the modalities for profiling the radionuclides over time is proposed. It should be noted that the development of such metrics is outside the scope of this work.

2.1 SELECTION CRITERIA

As part of the ultimate goal of nuclear fuel identification and monitoring, a preliminary investigation was performed into radionuclides that may be useful in the implementation of the strategy. The approach involved selection of candidate radionuclides out of over 200 from the chart of nuclides [11]. The selection criteria include:

- Non-actinide: Actinides exhibit complex behavior during irradiation.

- Gamma signature: The potential unique identifier should emit a unique signal that can be detected. In this case, unique is defined as the ease of positive detection by a radiation detector. It is important that no two

selected radionuclides have gamma energies close to each other. This will facilitate the resolution of the detected signals from the radionuclides.

- Medium to long half-life: A radioactive sample would decay completely in about 10 half-lives. Hence half-life of 10 years or more is desirable.

- Availability naturally or through synthesis: It is imperative that the radionuclide can be economically produced.

- High melting point: The physical form of the radionuclide needs to be preserved under reactor operating conditions.

- Small absorption cross section: Low cross section ensures that the radionuclide is not compromised via transmutation in the reactor environment.

2.2 SELECTED TAGGING MATERIAL

Table 2.1 provides the list of radionuclides that could potentially be used as the unique identifier. Seven radionuclides have been selected for the purpose of identification based on the criteria listed earlier. Ag108m was deleted from the list of potential identifiers due to its cross-section information's absence in the MCNP Data Libraries.

2.3 LIMITATIONS OF SELECTED MATERIAL

Some of these nuclides did not meet all the desired criteria. Table 2.2 shows a check list of the criteria each radionuclide met. Cs-137 has a very low melting point. This can be remedied by making the identifier a Cesium compound. An example is

Cesium Chromate (IV) which has a melting point of 982°C. All other radionuclides with melting point below 900°C could also be used in forms with high melting point. Examples include Barium Hexaboride and Europium Boride with melting point of 2070°C and 2600°C, respectively.

Table 2.1.List of potential radionuclides for the unique identifier
*: Value taken from JEFF 3.0/A Data

Nuclide	$T_{1/2}$ (years)	Gamma Emission (keV)	σ_γ (barns) @ 0.0253eV	Melting Point (°C)
Nb94	2.0×10^4	871.1	15.8	2477
		702.6		
Ag108m	420	722.9	50.7*	962
		433.9		
		614.3		
Cs137	30.07	661.7	0.25	28.5
		283.4		
Ba133	10.53	365	2.8	727
		81		
		302.9		
Eu152	13.54	121.8	12,796	822
		1408		
		344.3		
Eu154	8.59	123.1	1,353	822
		1274.5		
Ho166m	1.2×10^3	184.4	3,609	1472
		810.3		
		711.7		

Table 2.2 Checklist of the radionuclides that met each criterion

Criteria	Radionuclide						
	Nb94	Ag108m	Cs137	Ba133	Eu152	Eu154	Ho166m
Non-Actinide	✓	✓	✓	✓	✓	✓	✓
Unique Gamma Signature			✓	✓			
Half Life (≥10 years)	✓	✓	✓	✓	✓		✓
High Melting Point	✓	✓		✓	✓	✓	✓
Low Absorption Cross-Section			✓	✓			

All except Cs-137 and Ba-133 have significant absorption cross section at room temperature. Particularly for the holmium and europium nuclides, the cross sections are large enough for the samples to be denatured in a reactor environment [11]. It may be possible to shield these nuclides from thermal neutron absorption by encasing the finally fabricated identifier in a neutron shield such as cadmium foil. Cadmium-113 has a cross section of 20,600 barns which is 38% higher than that of Eu152, the largest cross section within the chosen radionuclides. It is expected that the cadmium case would cut off the thermal neutrons that would otherwise contribute to the transmutation of the identifiers.

Some radionuclides have gamma energies close to one another. For example, Eu-152 and Eu-154 have gamma signatures of 121.8 keV and 123.1 keV, respectively. Depending on detector resolution, these gammas may not be easily separated. However, both nuclides have other gamma signatures that are distinct enough for facilitated proper and unique identification. This is also the case for Nb-94, Ag-108m and Ho-166m with gamma energies 702.6 keV, 722.9 keV and 711.7 keV, respectively [11].

All selected nuclides except Eu-154 have half-lives greater than 10 years. Eu-154 with an 8.59 year half-life, would have measurable contribution to the identification of the nuclear fuel for more than 50 years [11]. Hence the half-life issue does not pose a significant adverse effect on the strategy being investigated.

3.   EFFECTIVENESS METRICS OF TAGGING MATERIAL

The two items that could compromise the effectiveness of the tagging material are signal interference from the spent fuel and transmutation susceptibility of the identifier. Each of these can compromise the integrity of the unique signal that is detected. It is necessary that the identifiers do not have any negative impacts on current reactor operations and safety standards as well. To determine the effect, it was necessary to compare the k_{eff} of the core with the identifier and without it.

3.1   SIGNAL INTERFERENCE

The depleted fuel in the core may contain either the same radionuclides which will be used as the identifier or different radionuclides which may have gamma signatures that are close to that of the identifier. Therefore if the signal from the spent fuel compromises the unique signal being emitted from the identifier, it would be difficult to distinguish the signals that are from the unique identifier. Figure 3.1 demonstrates how the extraneous signals from the fission products may interact with the unique signal from the identifier. Figure 3.1a shows how the external gamma signals from the spent fuel could contaminate the unique signal from the identifier and give an inaccurate reading in the detector. Figure 3.1b shows how the contamination of the unique signal could be avoided if the external signal was adequately shielded. This shielding could take the form of distance or some other physical barrier blocking the extraneous fuel signal.

To determine if the unique signal is compromised by the gamma rays coming from the depleted fuel, it was necessary to calculate the activity of each radionuclide after each time step using equation 3.1 [12]:

$$\alpha(t) = \alpha_0 e^{-\lambda t} \tag{3.1}$$

where, α_0 is the initial activity of the radionuclide in Becquerel (bq),

λ is the decay constant in sec^{-1} and

t is the elapsed time in sec.

Using the F4 tally in MCNPX, the neutron flux (cm^{-2}) is given for each expected gamma energy from the radionuclides of the identifier.
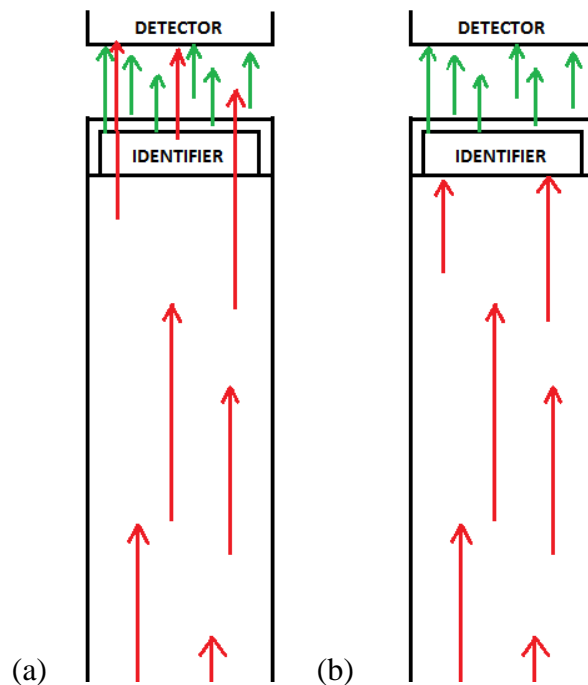

Figure 3.1 Spent fuel signal interfering with identifier signal. (a) Photons from the spent fuel compromising the unique signature of the identifier. (b) Photons from the spent fuel shielded from the unique signal of the identifier.

3.2 SUSCEPTIBILITY OF THE IDENTIFIER TO TRANSMUTATION

Since the signal is dependent upon the natural decay of the identifiers, it is important that the radionuclides are not compromised by transmutation. It is desirable that the decay of the radionuclides is dominated by natural decay rather than neutron absorption. To determine the dominating decay mode, the ratio of the reaction rate over the natural decay rate was used. Equation 3.2 gives the reaction rate and equation 3.3 gives the natural decay.

$$Reaction\ Rate = N\sigma_\gamma\Phi \qquad (3.2)$$

where, N is the atom density of the radionuclide in atoms/cm^3,

σ_γ is the radiative capture cross section in barns (b) and

Φ is the neutron flux is neutrons/cm^2-s.

$$Decay\ Rate = N\lambda \qquad (3.3)$$

Equation 3.4 gives the ratio of the reaction rate over the decay rate.

$$Decay\ Ratio = \frac{N\sigma_\gamma\Phi}{N\lambda} \qquad (3.4)$$

If the decay ratio is greater than 1, then the decay is mostly due to the reaction rate. If it is equal to 1, then the decay rate and reaction are equal. If it is less than 1, then the decay is mostly due to the decay rate. It is desirable that the decay ratio is less than one and is mostly due to natural decay.

The F4 tally multiplier in MCNPX was used to determine the reaction rate. The atom density (N) was calculated by MCNPX from the information available in the input file. The radiative capture cross section was obtained from the MCNP Data Libraries. The track length flux (φ) in cm^{-2} was obtained from the F4 tally. The product of the

output of the tally multiplier and the neutron intensity (neutrons/sec.) provides the reaction rate in disintegrations per seconds or Becquerel (Bq).

The neutron intensity is needed to obtain the flux in the radionuclides that would be used in the calculation of the reaction rate as can be seen in equation 3.5 [12].

$$\Phi = I\varphi \qquad\qquad 3.5$$

where, I is the neutron intensity in neutrons/sec and

φ is the track length flux in cm^{-2} from the F4 tally.

The average neutron intensity of the core was calculated in MCNPX for each time step.

3.2.1 Uncertainty Associated with Nuclear Cross Section Data. Many nations use their own evaluated nuclear data libraries. For example, China, Japan, and the USA use the Chinese Evaluated Nuclear Data Library (CENDL), Japanese Evaluated Nuclear Data Library (JENDL), and Evaluated Nuclear Data File (ENDF), respectively. Each library has a unique method for evaluating neutron cross sections for radionuclides which leads to discrepancies. Figure 3.2 shows the differences in radiative capture cross sections from multiple data libraries. For this reason, the cross section for a radionuclide could be different in each library. For instance, the method used to evaluate the total cross section for cesium-137 in JENDL 4.0 was to add all the partial cross sections together [13]. The partial cross sections, including radiative capture, were evaluated by use of the CCONE code, a code for nuclear data evaluation [13][14]. CASTHY, a neutron cross section statistical model, was use to evaluate the radiative capture cross section for cesium-137 in ENDF/B-VII.0 [15][16].
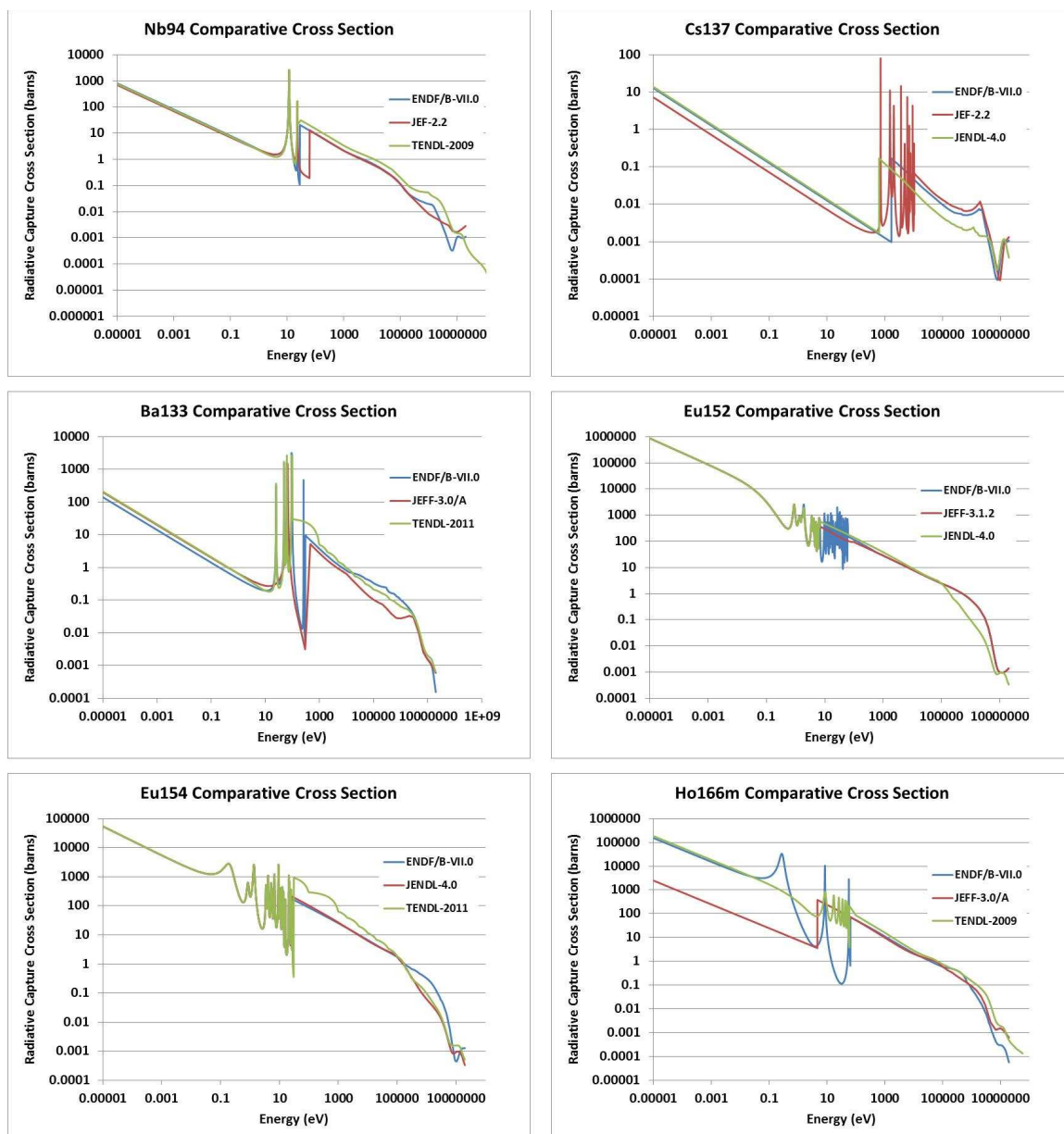
Figure 3.2 Comparative cross sections of each radionuclide from the identifier from various nuclear data libraries from Janis-3.4.

The tracking method proposed in this paper is based off of the information from ENDF/B VII.0 Library. The differences in cross section data for the libraries could have an impact on simulations. Simulations using different libraries may result in various transmutation rates for the selected tagging materials. This is the main cause of uncertainties in the results of simulations of this strategy. The uncertainties associated

with the cross section data is thus propagated to the transmutation analysis for the tagging radionuclides. It should be noted that the cross-section for some radionuclides is sometimes adopted from other data libraries. For this reason, some data libraries may have the identical cross section profiles for a radionuclide. For example, ENDF/B-VII.0 used the cross-section evaluation from JENDL 3.3 for Niobium-94 [17].

3.2.2 Thermal Neutron Flux. Using MCNP5, the flux in different parts of the core was obtained. The flux is used to determine the likelihood of the tagging material having interactions with the thermal neutrons. Figure 3.3 shows the flux per lethargy spectrum in the whole assembly, in the gas plenum, at the unshielded identifier location and shielded identifier location. The thermal neutron flux in the assembly is at least two orders of magnitude higher than the flux in the plenum. The flux at the unshielded identifier location is about two orders of magnitudes lower than the plenum flux. This indicates that far less thermal neutrons are getting to the identifier location then there are in the entire assembly or plenum. It is expected that there will be little interaction with the unshielded identifier because of the low thermal neutron flux in that location. This means that the identifiers are less likely to undergo transmutation. The earlier suggestion of encasing the identifiers in cadmium cover (see section 2.3) was evaluated. The resulting flux profile in the identifier location had the thermal neutrons completely cut-off as shown in Figure 3.3. This is an indication of the effectiveness of a cadmium shield in the mitigation of identifier transmutation via thermal neutron capture.

Figure 3.4 shows the cross section of each radionuclide with the flux spectrum in the identifier location over the neutron energy spectrum. The thermal neutron flux peaks at small neutron cross sections for Nb94, Cs137, and Ba133. Therefore, transmutation is

not expected for these radionuclides. The peak corresponds to high cross sections for Eu152, Eu154, and Ho166m. Some neutron interactions are expected in these radionuclides.
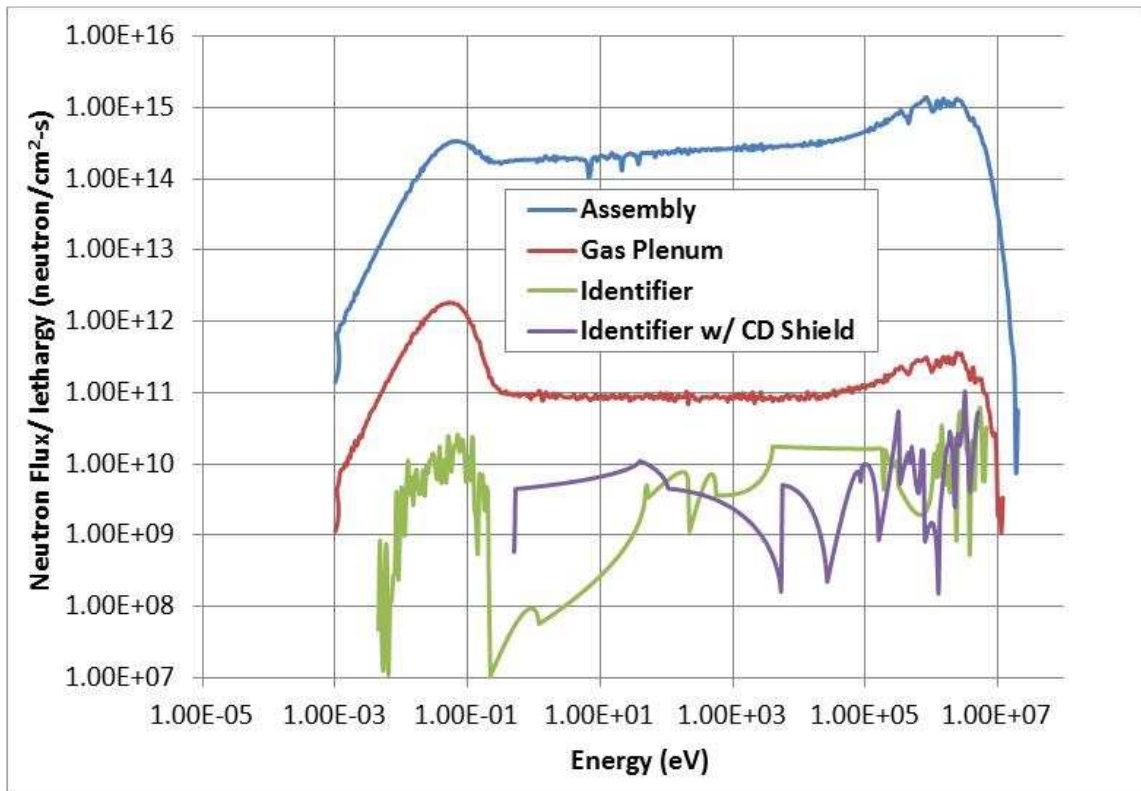
Figure 3.3 A comparison of the neutron flux in the fuel assembly, plenum, at the unshielded tagging material and shielded tagging material.

3.3   IMPACT OF TAGGING MATERIAL ON REACTOR OPERATION

It is desirable for the tagging material to have little effect on the reactor operations. To observe the effect of the tagging material on the reactor, the criticality was analyzed. The effective multiplication factor was compared between the core with the tagging material inside and the core without it. See Sections 4.2 to 4.4 for discussions.

Figure 3.4 Flux spectrum at the identifier location overlaid with the ENDF/B-VII.0 cross section of each radionuclide in the identifier.

4. ASSESSMENT OF PWR WITH TAGGED FUEL ASSEMBLIES

4.1. THE PWR MODEL

4.1.1 PWR Core Details. The geometry used for the fuel was cylindrical pellets with a diameter of 8.2 mm. The fuel pellets were modeled as one long pellet within the fuel 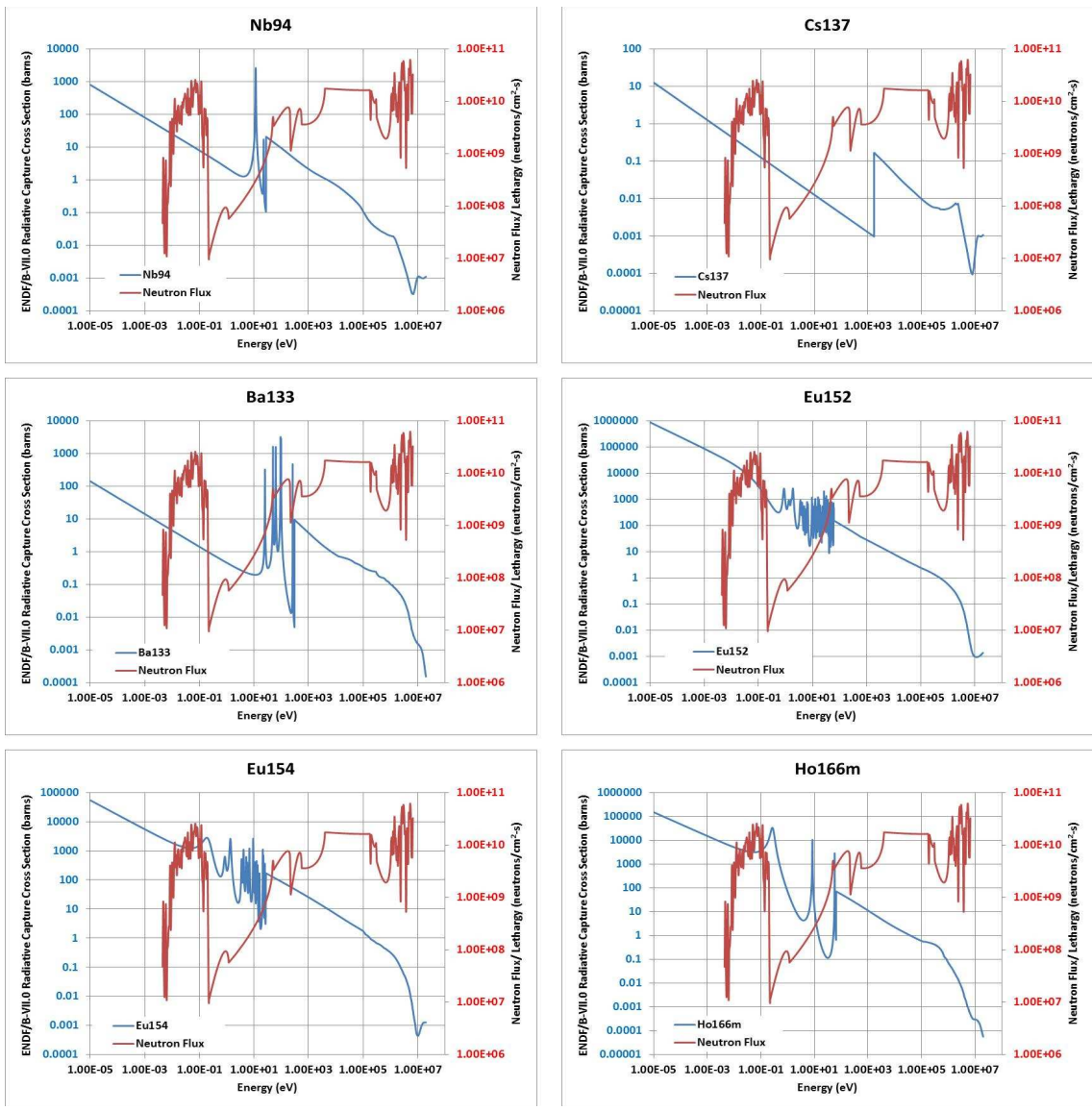pin with a length of 366 cm rather than individual pellets with a length of 13.5 mm each. The cladding material had a thickness of 0.57 mm with an outer diameter of 9.5 mm. Each individual fuel rod in an assembly had a rod pitch of 12.6 mm and a height of 400 cm. The reactor core contained 157 fuel assemblies with each assembly arranged in a 17 x 17 array. Out of the 289 fuel locations, there were 264 fuel rods in each assembly. The core diameter was 398.8 cm [10][18][19]. Table 4.1 gives the core design specifications. A top view of the model of the whole core is shown in Figure 4.1 using MCNPX Visual Editor Plotter Version X_24E. Figure 4.2 is a top view of a fuel assembly in the core. Figure 4.3 is the side view of the model showing the fuel pins with the fuel inside.

The fuel used in the reactor was uranium dioxide (UO_2) with a density of 10.41 g/cm^3 [12]. The fuel was enriched to 5%. Water was used as the moderator in the model and helium was used to fill the gap between the clad and pellets, as well as the plenum [18]. The cladding material was made up of ZIRLO whose composition was 98% zirconium, 1% tin, and 1% niobium [20].

Table 4.1 Core design specifications

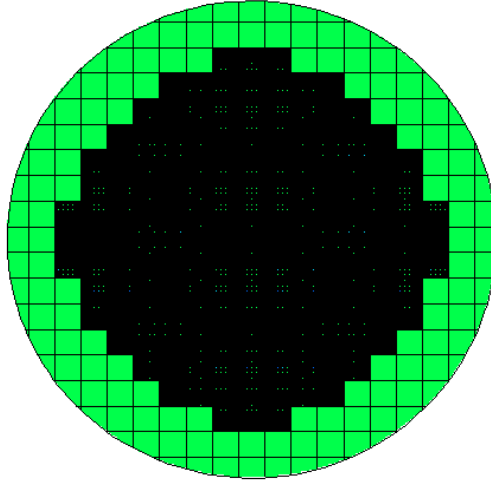| CORE DESIGN SPECIFICATIONS		
Temperature	573K	
Pressure	155 Bars	
Moderator	H_2O	
Coolant	H_2O	
Fuel	Chemical Form	UO_2
	Geometry	Cylindrical Pellets
	Diameter	8.2 mm
	Height	3.66 m
	Enrichment	5%
Fuel Pins	Cladding Material	ZIRLO
	Clad Thickness	0.57 mm
	Diameter	9.5 mm
	Height	4 m
Assembly	Geometry	17 x 17
	Pitch	12.6 mm
	# of Rod Locations	289
	# of Fuel Rods	264
Core	Diameter	3.988 m

Figure 4.1 x-y cross-sectional view of the core model in MCNPX Visual Editor Plotter Version X_24E. The detail of each fuel assembly above is shown in Figure 4.2.
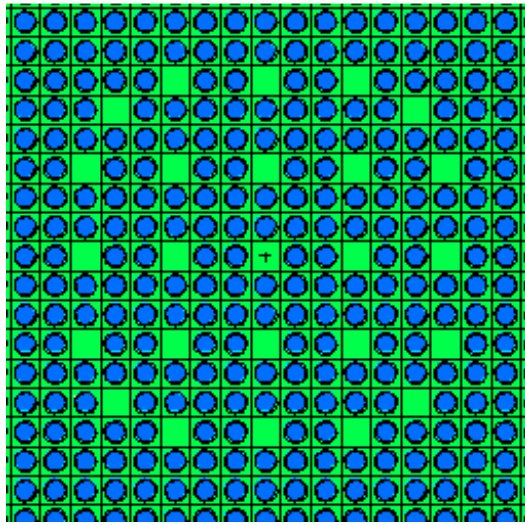

Figure 4.2 x-y cross-sectional view of the fuel assembly in MCNPX Visual Editor Plotter Version X_24E. Each assembly contains 264 fuel pins.
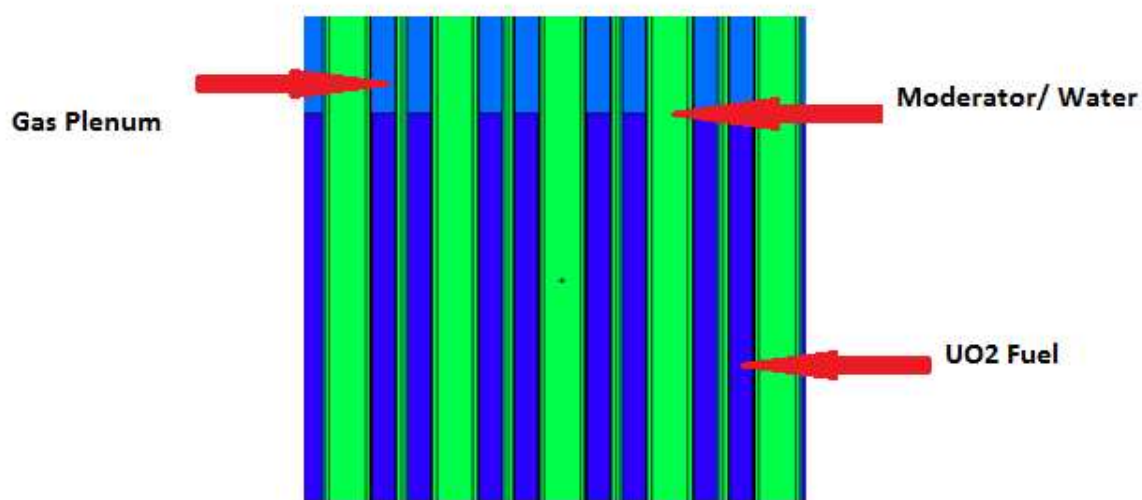
Figure 4.3 x-y cross-sectional view of the fuel assembly in MCNPX Visual Editor Plotter Version X_24E.

4.1.2 Tagging Material Placement. The identifiers (tagging radionuclides) that were used were arranged in a cylindrical wafer sized material with a 3 mm thickness. The diameter of the identifier was 8.2 mm. The 3 mm thickness of the identifier was made up of 0.5 mm thick layers of each identifier material as shown in Figure 4.4. The top of the identifier was located 0.5 mm from the top of the fuel pin. To keep the identifier in place at the top, an extra layer of 0.57 mm thick ZIRLO material was placed 3.5 mm from the top of the pin directly beneath the identifier.

4.2. REACTOR OPERATION CHARACTERISTICS - CHANGE IN k_{eff}

To determine if the tagging material changed the criticality of the core, the core was ran with the tagging material inside and ran without it. Figure 4.5 shows that there was little change between the profile with and without the tagging material. Overall, the tagging material had little effect on the criticality of the core. Figure 4.5 also shows the

change in core reactivity, $\Delta\rho$, due to the presence of the tagging material. The maximum positive reactivity change induced was at day 1900 with a value of 0.00185 ± 0.00256. The maximum negative reactivity change on the other hand was at day 2000 with a value of -0.00441 ± 0.00249. It should be noted that the reactivity effect is approximately consistent over the reactor operation period. The error bars on the change in reactivity at all the time steps are indicators of the consistency.
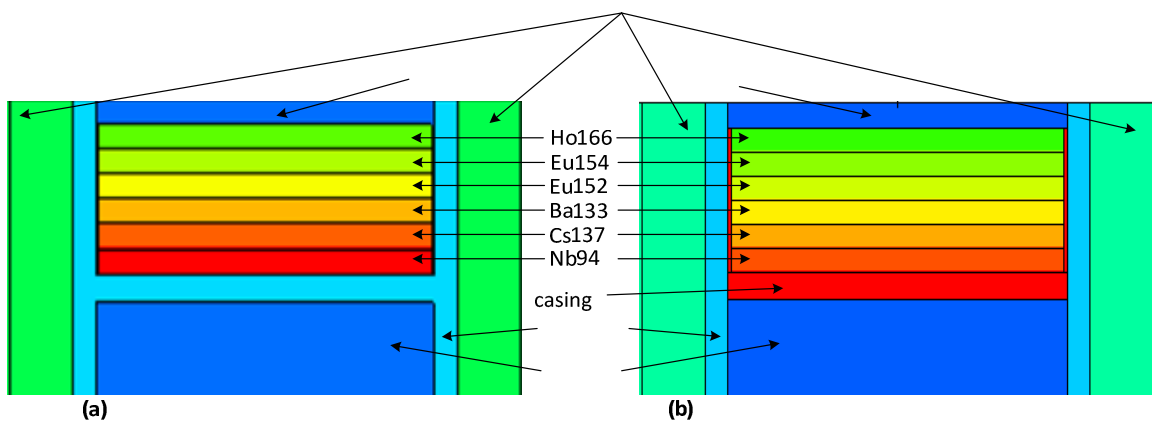
Figure 4.4 x-z cross-sectional view of the identifier in a fuel pin.
Each color represents a different identifier material.
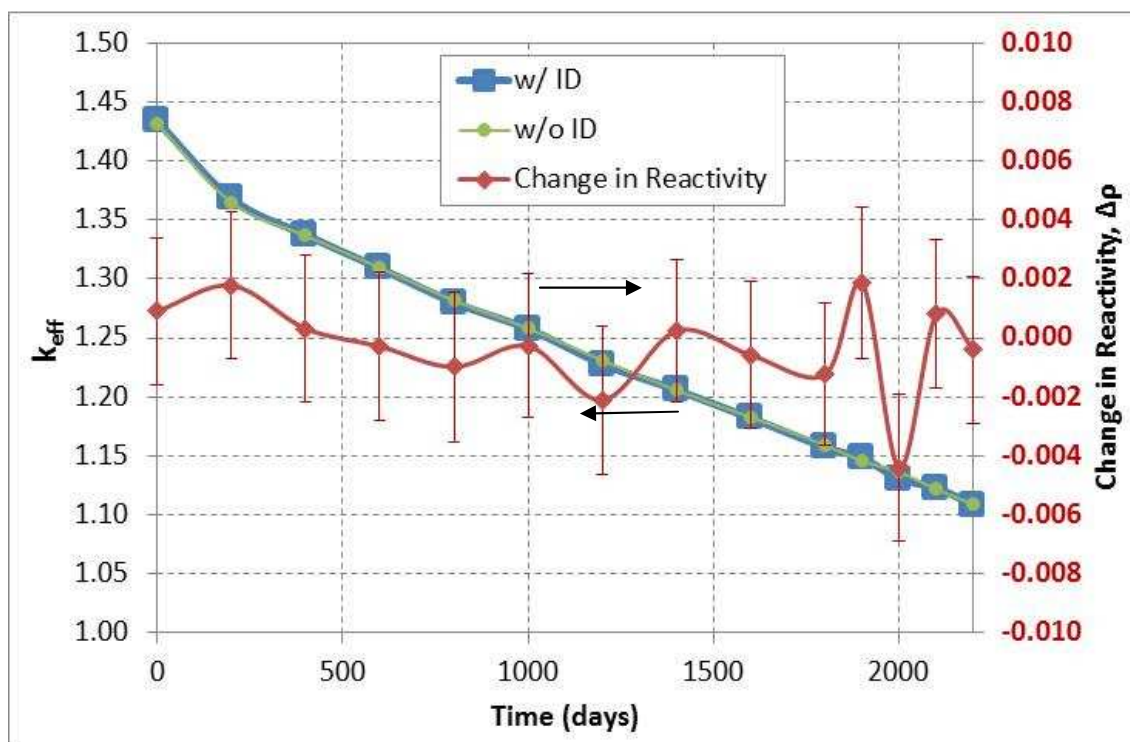
Figure 4.5 Criticality of the core with and without the tagging material over time and change in reactivity due to the tagging material.

4.3. TRANSMUTATION EFFECTS

In order to assess the impact of transmutation on the selected tagging radionuclides, the identifiers' concentrations were calculated at specific times over 2200 days of simulated reactor operation. These were compared with their concentrations in the case of decay-only scenario. This was done to evaluate the additional loss of the radionuclides by neutron capture and how the loss – if any – may impact the reliability of the signals generated by the tagging radionuclides.

In a decay-only scenario, the rate of change of the tagging material mass is given by

$$\frac{dm}{dt} = -\lambda m(t) \tag{4.1}$$

Where $m(t)$ is the mass of the radionuclide at any time t and λ is its decay constant. The solution to equation 4.1 is:

$$m(t) = m_0 e^{-\lambda t} \tag{4.2}$$

Where, m_0 is the initial mass of the radionuclide.

However, in a reactor environment the rate of change is also influenced by absorption reaction, the rate of change equation is:

$$\frac{dm}{dt} = -m(t)\left[\lambda + \int_{t'=t_0}^{t'=t} dt' \int_{All\ E} dE \int_{\vec{r}} d\vec{r}\ \sigma_a(E)\phi(\vec{r},E,t')\right] \tag{4.3}$$

Where $\sigma_a(E)$ is the energy dependent absorption cross section of the radionuclide and $\phi(\vec{r},E,t')$ is the neutron flux with energy E about location $\vec{r}$ in the reactor at time t'. Equation 4.3 assumed that none of the radionuclide may be transmuted to another amongst them. Nevertheless, the solution to the equation depends on the knowledge of the flux function $\phi(\vec{r},E,t')$. By using MCNPX for the simulation, this equation is solved to give $m(t)$ at the times steps specified.

It is convenient to designate the radionuclide concentration for the decay only calculation as $m_d(t)$ and the concentration which included transmutation effects as $m_x(t)$. It is expected that the additional loss due to transmutation would make m_x less than m_d. Hence we may characterize the transmutation effect, F_x by the fractional difference between m_d and m_x; so that:

$$F_x = \frac{m_d - m_x}{m_d} = 1 - \frac{m_x}{m_d} \qquad (4.4)$$

Ideally, it is desirable for F_x to be zero or as close to zero as possible. This would imply that the transmutation effect is negligible.

Figure 4.6 shows a transmutation effect for each radionuclide over the reactor operation time. The F_x value is close to zero for all time steps. The worst case of transmutation effect was on Eu152 at about 1.17%. This indicates that the loss of mass was mostly due to natural decay rather than through neutron interaction. Since the rate of decay for each radionuclide can be predicted, that characteristic could be used as a way to identify the fuel. Through a combination of concentration ratios of the radionuclides, unique signals can be made. A change of concentration in even one radionuclide denotes a new identifier. It should be noted that the transmutation effect was evaluated without cadmium shield around the identifiers. With a cadmium shield effectively cutting off the thermal neutrons (see Figure 3.3), the transmutation effect should be mitigated with a cadmium shield. Recall that the thermal neutron absorption cross section of Cd113 is 38% higher than that of Eu152. Given that only 1.17% of the transformed Eu152 is via neutron absorption, then the loss of Cd113 via neutron absorption in the same flux exposure should be about 38% higher. It is expected that the cadmium should not be completely depleted during the period of irradiation.
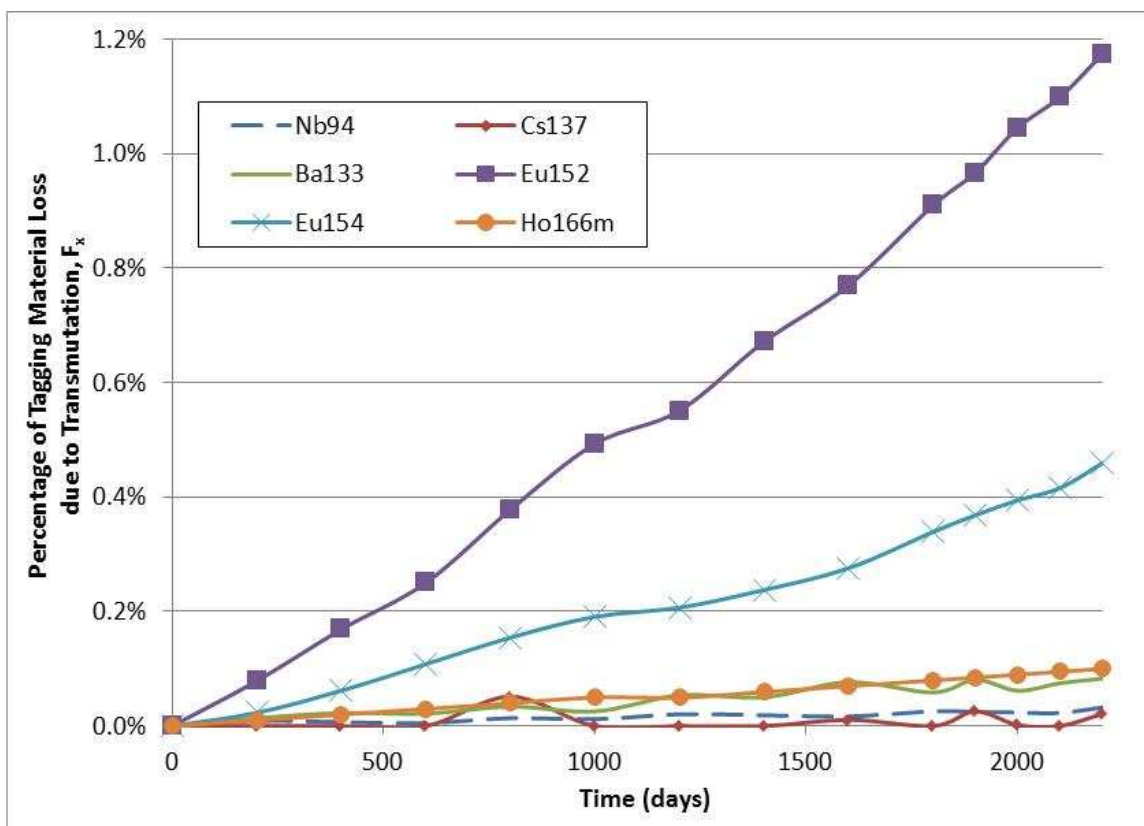
Figure 4.6 Percentage of tagging material lost over time due to transmutation.

4.4 EFFECT OF FISSION PRODUCTS ON IDENTIFIER SIGNAL DETECTION

Figure 4.7 compares the gamma spectrum of the identifier material at the beginning-of-cycle (BOC) of the core, end-of-cycle (EOC) of the core, and after 30 days post-irradiation. The BOC starts at day 0 when the core starts to burn the fuel, and the EOC is at day 2200 when the core stops burning. Fresh UO_2 was placed in the core at BOC. Therefore, it is not expected that any signal from the UO_2 should interfere with the signal from the tagging material. At the EOC, the peaks are noticeably higher compared to the peaks at the BOC. This indicates that the signal from the tagging material will be compromised by the signal from the spent fuel. From Figure 4.7, the external signals increases after 30 days of decay; an increase attributable to the beta decay fission

products with the same atomic mass as the selected radionuclides but with lower proton number. For these fission products to improve their proton-to-neutron number ratio, they decay towards higher proton numbers, thereby resulting in the increase in abundance of the selected radionuclides in the fission product inventory in the spent fuel. Nb94 signal intensity increased by 175% at EOC and 478% 30 days post-irradiation. Cs137 saw an increase of 12% and 89% at EOC and 30 days post-irradiation, respectively. Ba133 signal intensity increased by 25% at EOC and 111% post-irradiation. Eu152 saw an increase of 46% at EOC and 209% post-irradiation. Eu154 signal intensity increased by 1260% at EOC and 4545% post-irradiation. Ho166m saw an increase 200% at EOC and 379% post-irradiation. The changes in signal intensities are summarized in Table 4.2. The contribution of the external signals could be mitigated by shielding the tagging material from the spent fuel signal with a material such as lead. Another approach to mitigate this issue is signal refinement through the use of fission product yield curve to isolate signal contribution from the fission products. A combination of the two approaches may be employed for better result.
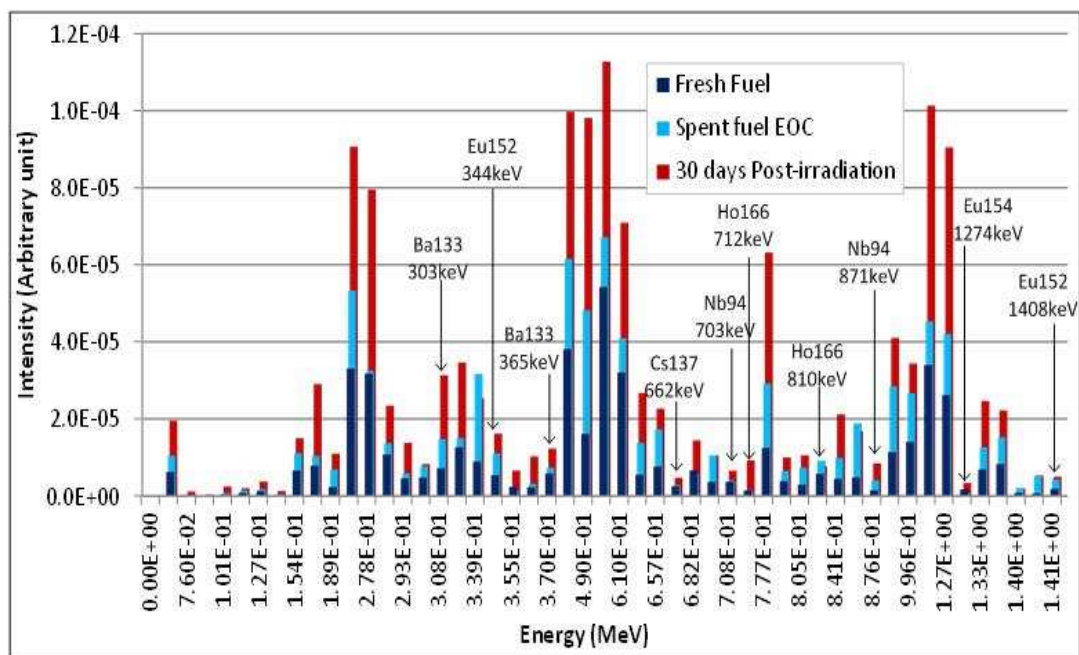
Figure 4.7 Gamma spectrum of the tagging material at the beginning of cycle, the end of cycle, and 30 days post-irradiation.

Table 4.2 Change in signal intensity at EOC and 30 day post irradiation.

E (keV)	Nuclide	Signature	Change in signal intensity (%)	
			EOC	30d Post-Irr.
81	Ba133	Secondary	242.96	397.86
122	Eu152	Primary	45.59	209.10
123	Eu154	Primary	1259.61	4544.81
184	Ho166m	Primary	199.97	378.54
283	Cs137	Secondary	27.52	117.84
303	Ba133	Tertiary	104.06	333.92
344	Eu152	Tertiary	104.47	199.98
365	Ba133	Primary	25.01	111.11
662	Cs137	Primary	11.75	89.27
703	Nb94	Secondary	8.38	78.17
712	Ho166m	Tertiary	4.66	557.56
810	Ho166m	Secondary	58.43	34.36
871	Nb94	Primary	175.33	478.44
1275	Eu154	Secondary	-47.10	94.44
1408	Eu152	Secondary	133.36	171.35

5. CONCLUSION

After reviewing over 200 radionuclides, six have been selected for the purpose of identifying fuel assemblies:

- Nb94: Metallic element, Melting Point=2477°C, σ_γ @ 0.0253 eV= 15.8 barns, $T_{1/2}$=2.0x10^4 years.

- Cs137: Metallic element, Melting Point=28.5°C, σ_γ @ 0.0253 eV= 0.25 barns, $T_{1/2}$=30.7 years.

- Ba133: Metallic element, Melting Point=727°C, σ_γ @ 0.0253 eV= 2.8 barns, $T_{1/2}$=10.53 years.

- Eu152: Metallic element, Melting Point=822°C, σ_γ @ 0.0253 eV= 12,796 barns, $T_{1/2}$=13.54 years.

- Eu154: Metallic element, Melting Point=822°C, σ_γ @ 0.0253 eV= 1,353 barns, $T_{1/2}$=8.59 years.

- Ho166m: Metallic element, Melting Point=1472°C, σ_γ @ 0.0253 eV= 3,609 barns, $T_{1/2}$=1.2x10^3 years.

They were chosen based on the following criteria:

1. non-actinide

2. detectable gamma signature

3. medium to long half-life

4. natural existence or ease of synthesis

5. high melting point

6. small absorption cross section.

Some of the selected radionuclides did not satisfy all criteria, but are deemed to have possible remedy to the short-comings. For example, ^{137}Cs has a very low melting point, which may be remedied by making the tagging material a Cesium compound such as Cesium Chromate (IV) with a melting point of 982°C. Another example is the case of Europium and Holmium radionuclides with cross sections up to 13,000 barns at 0.0253eV. The effects of the huge thermal cross sections may be mitigated by encasing the tagging materials in other materials with high thermal neutron absorption.

A whole core model of a typical PWR was developed in MCNP. This model was used as the basis for the evaluation of the performance of the tagging materials in the core as well as their impact on reactor operation. The results indicated that there is negligible impact of the tagging materials on the reactor operation. The maximum positive reactivity change induced was at day 1900 with a value of 0.00185 ± 0.00256. The maximum negative reactivity change on the other hand was at day 2000 with a value of -0.00441 ± 0.00249. In addition the effect of transmutation on the depletion of the tagging material is negligible. The maximum transmutation effect noted is 1.17% in Eu152. Hence it was concluded that the decay profile of the radionuclides is sufficient to reconstruct the initial concentrations of the radionuclides, thus characterizing the fuel being monitored. A cadmium shield could also be used to mitigate some of that transmutation effect by effectively cutting off the thermal neutrons. It was found that the

signal from the tagging material will be compromised at the core EOC and beyond, due to extraneous signals from the spent fuel. This could be mitigated via shielding and signal refinement. It was noted that at EOC, the maximum change in intensity was 1260% which occurred in Eu154. Cs137 saw the minimum change of 12%. At 30 days post-irradiation, Eu154 saw the maximum change in signal intensity of 4545%. Cs137 saw the minimum change of 89%.

Future effort on this project may include development of tagging schemes for unique identification, sensitivity and uncertainty analysis for the reconstruction of the initial radionuclide concentration. In addition further work could be done to optimization of extraneous signal shielding, and develop schemes for signal refinement since the success of the proposed strategy depends on the ability to profile the radionuclides used as identifiers.

BIBLIOGRAPHY

[1] E. S. Lyman, "The Global Nuclear Energy Partnership: Will it Advance Nonproliferation or Undermine It?" Global Security Program.

[2] "International Framework for Nuclear Energy Cooperation (formerly Global Nuclear Energy Partnership)" World Nuclear Association, July 2012.

[3] P. P. Craig and J. A. Jungerman, *The Nuclear Arms Race: Technology and Society*, McGraw-Hill College, 1990.

[4] U.S. Department of State, "<http://www.state.gov/t/isn/npt/,>" Accessed 3 May, 2013.

[5] World Nuclear Association, "Safeguards to Prevent Nuclear Proliferation," April 2012.

[6] S. DeMuth and D. Lockwood, "Safeguards by Design (SBD) for the Next Generation Safeguards Initiative (NGSI)," IAEA Safeguards Symposium, Vienna, Austria, 2010.

[7] R. G. Cochran and N. Tsoulfanidis, *The Nuclear Fuel Cycle: Analysis and Management 2nd Edition*, American Nuclear Society, La Grange Park, IL 60525, 1990.

[8] European Nuclear Society, "<http://www.euronuclear.org/info/encyclopedia/n/npp-reactor-types.htm,>" Accessed 3 May, 2013.

[9] International Atomic Energy Agency, "50 Years of Nuclear Energy," <http://www.iaea.org/About/Policy/GC/GC48/Documents/gc48inf-4_ftn3.pdf,> Accessed 3 May, 2013.

[10] US Nuclear Regulatory Commission "AP1000 Design Control Document".

[11] E. M. Baum, M. C. Ernesti, H. D. Knox, T. R. Miller, and A. M. Watson, *Nuclides and Isotopes: Chart of the Nuclides 17th Edition*, Bechtel Marine Propulsion Laboratory, (2010).

[12] J. R. Lamarsh and A. J. Baratta, *Introduction to Nuclear Engineering 3rd Edition*, Prentice-Hall Inc., Upper Saddle Rive, NJ 07458.

[13] N. Iwamoto "Jendl-4.0 Incident Neutron Data" JANIS 3.4 OECD Nuclear Energy Agency.

[14] O. Iwamoto, "Development of a Comprehensive Code for Nuclear Data Evaluation, CCONE, and Validation Using Neutron-Induced Cross Sections for Uranium Isotopes," Journal of Nuclear Science and Technology, Vol. 44, No. 5, p. 687–697 (2007).

[15] JNDC FP Nuclear Data W.G. "Jendl-4.0 Incident Neutron Data" JANIS 3.4 OECD Nuclear Energy Agency.

[16] Nuclear Energy Agency, "<http://www.oecd-nea.org/tools/abstract/detail/nea-1395/,>" Accessed 2 April, 2013.

[17] Nuclear Data Services- International Atomic Energy Agency, "<http://www-nds.iaea.org/point2007/1KEV/ZA041094,>" Accessed 2 April, 2013.

[18] N. E. Todreas and M. Kazimi, *Nuclear Systems Volume I: Thermal Hydraulics Fundamentals*, Hemisphere Publishing Corporation, 1990.

[19] Westinghouse Electric Co. LLC, "The Westinghouse AP1000 Nuclear Plant: Plant Description" 2003.

[20] M. Steinbruck and M. Bottcher, "Air Oxidation of Zircaloy-4, M5 and ZIRLO Cladding Alloys at High Temperatures" Journal of Nuclear Materials, Vol. 414 Issue 2, July 15, 2011, p. 276-285.

VITA

Aaron Peterson was born in Houston, Texas. He graduated from Tuskegee University in May 2011 with a bachelor degree in aerospace engineering. While at Tuskegee University, he worked at The Tuskegee Center of Advanced Materials (T-CAM) and was active in the American Institute of Aeronautics and Astronautics (AIAA) chapter. The summer of 2011 was spent working for the Tennessee Valley Authority as an intern. He enrolled at Missouri S&T in the fall of 2011 to pursue a master in nuclear engineering. He completed his master degree in the summer of 2013.